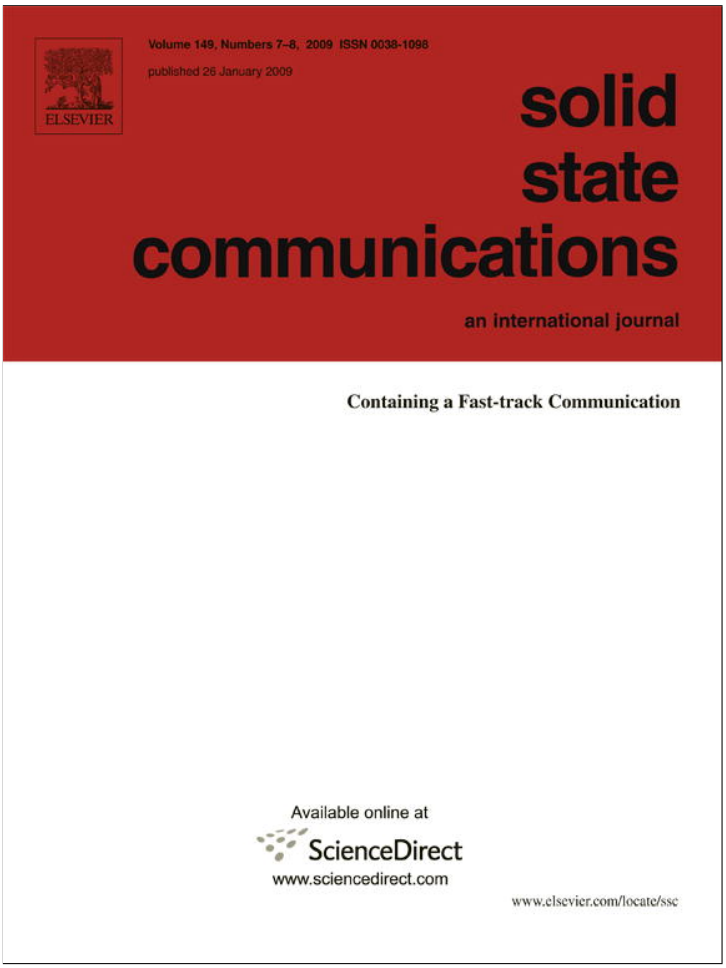

Solid State Communications 149 (2009) 315–318

Contents lists available at ScienceDirect

Solid State Communications

journal homepage: www.elsevier.com/locate/ssc

Preparation of one dimensional Bi_2O_3-core/ZnO-shell structures by thermal evaporation and atomic layer deposition

Sunghoon Park, Jina Jun, Hoyun Woo Kim, Chongmu Lee *

Department of Materials science and Engineering, Inha University, Incheon 402-751, South Korea

ARTICLE INFO

Article history:
Received 8 May 2008
Accepted 24 November 2008 by R. Phillips
Available online 7 December 2008

PACS:
61.46.-w
78.55.-m
81.07.-b

Keywords:
A. Bi_2O_3
A. ZnO
C. One-dimensional structure
D. Thermal evaporation

ABSTRACT

One dimensional(1D) Bi_2O_3-core/ZnO-shell structures with uniform layer thicknesses were prepared by using a two step process consisting of thermal evaporation of Bi_2O_3 and ALD of ZnO. Highly straight 1D Bi_2O_3 structures were synthesized by thermal evaporation of Bi powders on c-plane Al_2O_3 substrates and then ZnO layers were coated on them by ALD.

SEM analysis shows that the oxygen partial pressure must be precisely controlled to obtain straight Bi_2O_3 nanowires. According to the TEM analysis results the Bi_2O_3-core is a pure tetragonal β-Bi_2O_3 phase single crystal, while the ZnO-shell is amorphous. Photoluminescence (PL) measurement of the ID core/shell nanostructures under excitation at 325 nm indicates that the critical number of ALD cycle for which a transition from a violet emission characteristic of Bi_2O_3 to UV and green–yellow emissions characteristic of ZnO occurs is less than 10, suggesting that the wavelength of the emission changes abruptly with an increase in the number of ALD cycle.

1. Introduction

Radial core-shell heterostructure in which the heterointerface is parallel to the wire axis is one of the two basic nanowire heterostructures together with axial heterostructures in which the heterointerface is perpendicular to the wire axis. There are many important reasons to make efforts to form controlled radial heterostructures. One reason is protection of nanowires from contamination or oxidation and passivation of interface states abundant at the surface of nanowires which have a very large surface-to-volume ratio [1]. Another is to give various functions which can be effectively used for nanoscale electronic or optoelectronic devices [2]. A dielectric shell could provide electrical isolation. A shell dielectric could be used to form a high-quality optical cavity around a small core nanowire acting as the gain medium in nanowire FET applications. A dissimilar semiconductor shell could be used to generate internal fields perpendicular to the interface to provide confinement potentials for carriers in either the core or the shell. By combining a radial heterojunction with a layer of dopant atoms, a two-dimensional cylindrical quantum well with high-mobility change carriers could be made. A ferroelectric oxide shell offers the opportunity to make nonvolatile RAM or tunable transceivers [2]. Furthermore, as demand for fabricating special nanowire structures increases, development of methods not only for synthesizing a wide variety of nanowires but also for modifying or improving the properties of as-synthesized nanowires is becoming increasingly important. For example, the wavelength of the light emitting from a radial core/shell nanowire structure could be controlled by selecting proper materials and thicknesses for the core and the shell.

Bismuth oxides are attractive materials owing to their special physical properties such as significant energy band gap, high refractive index, dielectric permittivity, and high oxygen-ion conductivity, as well as marked photoconductivity and photoluminescence. These peculiar features make the bismuth oxides applicable to sensors, optical coatings, photovoltaic cells, microwave integrated circuits, transparent ceramic glass manufacturing, cathode ray tubes [3]. They are also used as the soft oxidation of hydrocarbons and good electrolyte materials for the applications such as solid oxide fuel cells and oxygen sensors [4]. The 1D nanostructures of bismuth oxide have been prepared by using various techniques such as hydrothermal synthesis, microemulsion, metal-organic chemical vapor deposition, the chemical method, the oxidative metal vapor transport deposition, the template-based heat treatment, thermal oxidation [5]. However, to the best of own knowledge, Bi_2O_3 nanowires have never been successfully synthesized by using thermal evaporation which is known as the simplest and commonest method for preparation of 1D nanostructures. Furthermore, no radial 1D structure with a Bi_2O_3 core has been reported before. In this paper, we report on preparation of 1D

* Corresponding author. Tel.: +82 32 8607536; fax: +82 32 8737537.
E-mail address: cmlee@inha.ac.kr (C. Lee).

0038-1098/$ – see front matter © 2008 Elsevier Ltd. All rights reserved.
doi:10.1016/j.ssc.2008.11.037

nanostructures of Bi_2O_3-core/ZnO-shell by using a two-step process of thermal evaporation of Bi_2O_3 and atomic layer deposition (ALD) of ZnO.

2. Experimental

Preparation of Bi_2O_3-core/ZnO-shell basically consists of two steps: synthesis of Bi_2O_3 nanowires by using thermal evaporation and coating of the Bi_2O_3 nanowires with ZnO thin films by using ALD. First, the gold(Au)-coated Al_2O_3(0001) substrate was put on top of an alumina boat loaded with pure Bi powders positioned at the center of a quartz tube furnace. The furnace was ramped up to 900 °C and maintained the temperature for 2h with an ambient gas ($Ar + O_2$) held at a constant total pressure of 2 Torr. Next, the Si substrate with the as-synthesited Bi_2O_3 nanowires was transferred to an ALD chamber. Diethylzinc(DEZn) and H_2O were alternately fed into the chamber through separate inlet lines and nozzles. Typical pulse times were 0.2, 0.2 and 2 s for DEZn feed, H_2O feed, and the reactants purge, respectively. The details of the sample preparation procedures and the experimental set-ups are described elsewhere.

The morphology and size of the final products were examined using scanning electron microscopy (SEM, Hitachi S-4200). Glancing angle (0.5°) X–ray diffraction (XRD) analysis was performed to investigate the phases of the obtained products. High resolution transmission electron microscopy (HRTEM) and selected area electron diffraction (SAED) were carried out on Philips CM-200 electron microscope at an acceleration voltage of 200 kV. The samples used for characterization were dispersed in absolute ethanol and ultrasonicated before SEM and TEM observations. The photoluminescence (PL) measurement was conducted at room temperature by using a He–Cd laser (325 nm) as an excitation source.

3. Results and discussion

Figs. 1(a) and (b) display SEM images of the as–synthesized Bi_2O_3 nanowires on Si(100) and Al_2O_3(0001) substrates, respectively. We can see a distinct difference between the two SEM images. The nanowires grown on the Si(100) substrate are much shorter than those on the Al_2O_3(0001) substrate. Also many Bi_2O_3 particles are seen on the Al_2O_3 substrate surface, which suggests following two things :

(1) Bi_2O_3 nanowires nucleate and grow as particles at the substrate surface first and then grow in a length direction.
(2) The growth rate of Bi_2O_3 nanowires is much lower on the Si(100) substrate than on the Al_2O_3(0001) substrate.

As is well known, thermal evaporation is the most widely used technique in synthesizing nanowires of various materials. A variety of oxide nanowires have been reported to be synthesized by using the thermal evaporation technique, yet there has been almost no report on the growth of Bi_2O_3 nanowires by thermal evaporation. β-Bi_2O_3 has a tetragonal structure with lattice constants $a = 5.63$ Å and $c = 7.74$ Å whereas Al_2O_3 has a hexagonal close-packed structure with lattice constants $a = 4.76$ Å and $c = 12.99$ Å. The mismatch between the c of β-Bi_2O_3 (5.63 Å) and the a of Si (5.43 Å) is only 3.6%, while that between the c of β-Bi_2O_3 (5.63 Å) and the a of Al_2O_3 (4.76 Å) is 15.5%. Hence, Al_2O_3 has much larger lattice mismatch with β-Bi_2O_3 than Si. Therefore, Al_2O_3 has not been considered as a candidate for a substrate material for Bi_2O_3 nanowire growth based on thermal evaporation of bismuth or bismuth oxide powders, which may be the reason why synthesis of Bi_2O_3 nanowires by using a thermal evaporation method has not been successful yet. It is not understood at the moment why the growth rate of Bi_2O_3 nanowires is far lower on the Si substrate than on the Al_2O_3 substrate. According to the capillarity theory for heteronucleation [6], the energy barrier for nucleation decreases and thus the nucleation rate increases as the wettability between a condensate and a substrate increases. There must be a factor in the Bi_2O_3–Al_2O_3 binary system other than lattice mismatch that enhances wettability between Bi_2O_3 nuclei and the Al_2O_3 substrate.

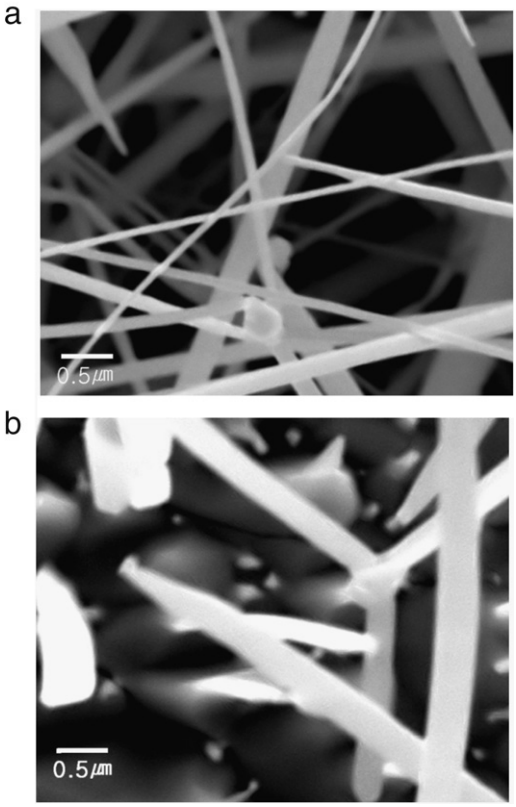

Fig. 1. SEM images of Bi_2O_3 nanowires grown by thermal evaporation at 550 °C with the oxygen partial pressure fixed at 1.5% (a) on (0001) Al_2O_3 and (b) on (100) Si.

A quantitative analysis of chemical compositions was performed by EDS point scanning on Fig. 2 shows that element Au as well as Bi and O exist, indicating that the spherical nanoparticles at the tip of nanowires are composed of Au, Bi, and O components. The existence of Au in the nanoparticles is an evidence that the growth of the Bi_2O_3 nanowire is via VLS mechanism. The growth mechanism of one-dimensional nanostructures could be different for different process parameters. Particularly it depends on the growth temperature. The VLS mechanism in which ID structures grow with an assistance of catalysts is dominant at lower temperatures because thermal energy is not enough for the nucleation and growth of the structure. In contrast, the VS mechanism is dominant at a higher temperatures where sufficient thermal energy is provided. As the process parameters for the Bi_2O_3 nanowire growth in this work is basically the same as those in our work for other nanowire growth, there is no reason why the growth mechanism differs.

The structure and phase purity of the products were examined by XRD. Fig. 3 shows a typical XRD pattern of the as-synthesized samples at 550 °C for 2 h. All the reflection peaks except two Au-related peaks due to the Au catalyst can be readily indexed to the tetragonal β-Bi_2O_3 with lattice constants $a = 7.742$ Å and $c = 5.631$ Å (JCPDS 78-1793). No other phase except Au used as a catalyst was detected in Fig. 4 indicating the high purity of the final products. As is well known, α-Bi_2O_3 is the only low temperature phase, while β-, γ-, and δ-Bi_2O_3 [7] and ω-Bi_2O_3 [8] are high temperature structures. It is known that tetragonal β-Bi_2O_3 with a distorted defect-fluorite structure

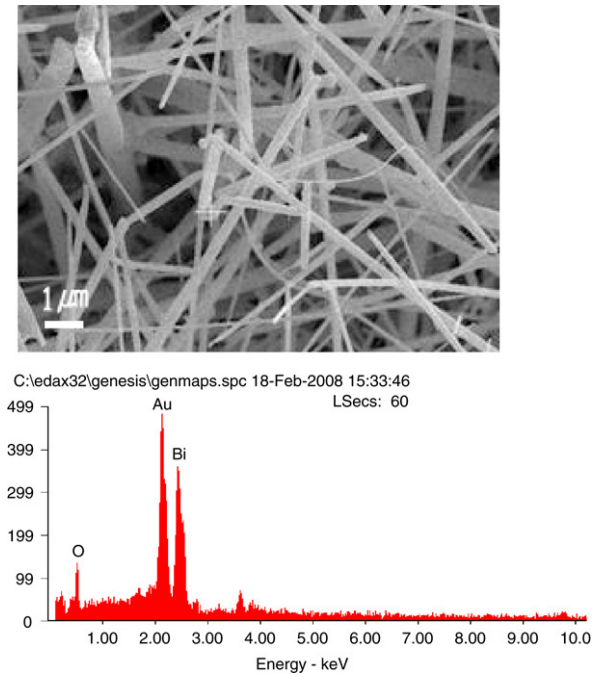

Fig. 2. An EDS spectrum at the tip of a Bi_2O_3 nanowire.

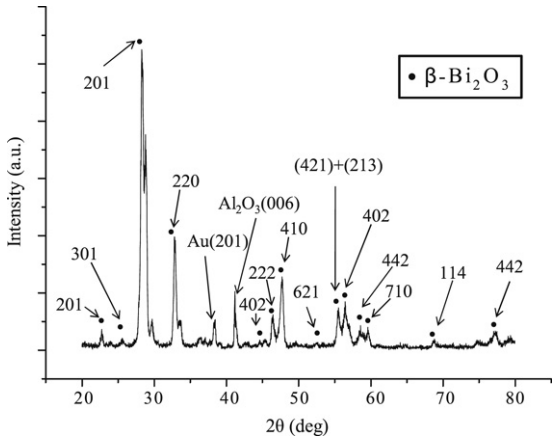

Fig. 3. The XRD pattern of the Bi_2O_3 nanowires grown by thermal evaporation on (0001) Al_2O_3 at 550 °C at an oxygen partial pressure of 1.5%.

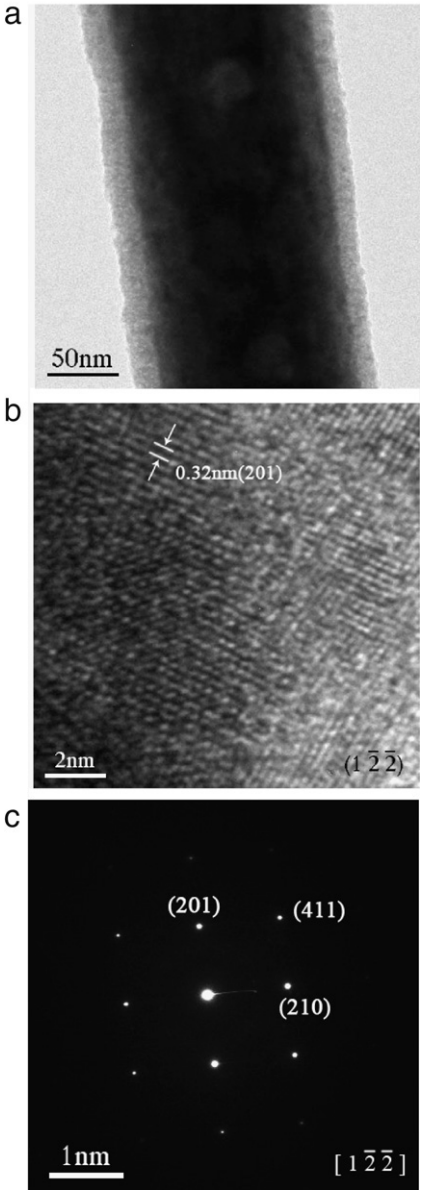

Fig. 4. (a) TEM image, (b) HRTEM image and (c) SAED pattern of a Bi_2O_3-core/ZnO-shell nanowire structure.

transforms into stable monoclinic α-Bi_2O_3 at about 870 K [9]. Formation of tetragonal β-Bi_2O_3 at 923 K on cooling cubic δ- Bi_2O_3 has been reported to be observed before [10]. In the case of our products β-Bi_2O_3 seems to exist as a metastable phase at room temperature. The dominant crystal structure of Bi_2O_3 nanowires at ambient conditions reported as yet is α-Bi_2O_3. The Bi_2O_3 nanowires synthesized by using hydrothermal [11], chemical [12], metal organic chemical vapor deposition (MOCVD) [13] and atmospheric pressure CVD techniques [14] was reported to have an α-Bi_2O_3 phase, while Bi_2O_3 nanotubes synthesized by oxidizing the bismuth nanotubes or nanowires in air [15] and Bi_2O_3 nanowires synthesized by using an oxidative metal vapor transport deposition technique [16] to have β-Bi_2O_3 phase. On the other hand, Kumari et al. [17] reported that one-dimensional nanowires and nanoflowers of Bi_2O_3 synthesized by using an oxidative metal vapor transport deposition technique had both α- and β-Bi_2O_3 phases. Judging from these reports and our results in this work, we may conclude that Bi_2O_3 nanowires have a stable α-Bi_2O_3 or metastable β-Bi_2O_3 phase depending on the synthesis method or the synthesis process conditions.

Fig. 4(a) is TEM image of a Bi_2O_3-core/ZnO-shell nanowire structure prepared by a two-step process consisting of thermal evaporation of Bi powders in an oxygen atmosphere at 900 °C and atomic layer deposition of ZnO at 170 °C using DEZn and H_2O as a precursor of Zn and an oxidant, respectively. This TEM image clearly displays that a Bi_2O_3-core with a diameter of about 130 nm is surrounded by a ZnO-shell with a thickness of 15–20 nm. The thicknesses of the Bi_2O_3-core and the ZnO-shell are uniform all the way along the nanowire length direction. High-resolution TEM(HRTEM) images (Fig. 4(b)) and selected area electron diffraction (SAED) patterns (Fig. 4(c)) recorded from the core layer reveal that an individual Bi_2O_3 nanowire core is a single crystal of the tetragonal structure with lattice constants $a = 7.742$ Å and $c = 5.631$ Å and Bi_2O_3 nanowires grow along the (101) direction. From the HRTEM image, clear lattice fringes perpendicular to the nanowire length direction are observed, indicating that the nanowire is of a single crystalline nature. The interplanar spacing is 0.32 nm, which is corresponding to the (201) crystallographic plane of the tetragonal β-Bi_2O_3 lattice. The associated SAED pattern (Fig. 4(c)) recorded, with the incident

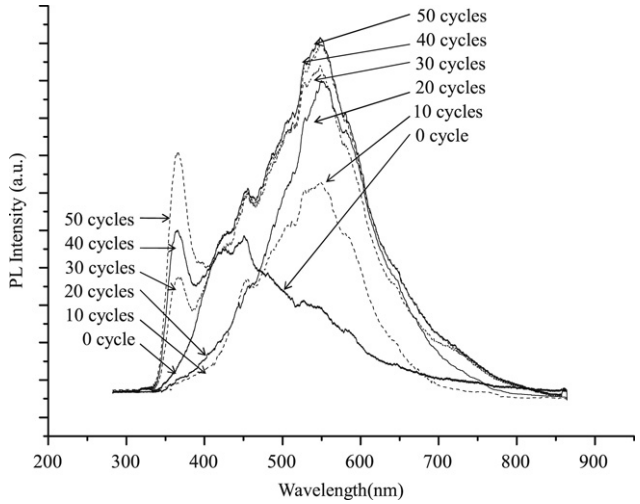

Fig. 5. A PL spectrum of the nanowires grown by thermal evaporation on (0001) Al_2O_3 at 550 °C at an oxygen partial pressure of 1.5%.

electron beam parallel to the (010) direction and perpendicular to the nanowire length direction was indexed for the [1 2 $\bar{2}$] zone axis of the crystalline β-Bi_2O_3. The well defined SAED pattern confirms that the Bi_2O_3 nanowire is monocrystalline. Differently from the Bi_2O_3-core, the ZnO-shell seems to be amorphous as no fringe pattern is observed in the ZnO shell area of the TEM image.

Fig. 5 represents the room temperature PL spectra of 1D Bi_2O_3-core/ZnO-sell structures. For the 0 cycle of ZnO ALD corresponding to the Bi_2O_3 nanowire not coated with ZnO at all, there exist a broad emission band with a main peak centered around 450 nm and a shoulder at a bout 425 nm, in the blue region. A 324nm He–Cd laser was used as an excitation source for the PL. Similar blue emissions were observed for Bi_2O_3 nanonods synthesized by authors using an MOCVD technique and Bi_2O_3 nanoparticles synthesized using a microemulsion technique [18]. On the other hand, there is also a recent report that broad PL peaks centered at around 588.6 and 598.7 nm obtained for Bi_2O_3 structures seems to be related to the electrovalency of Bi ions [19]. It is known that the emission of Bi ion is assigned to its electrovalency, which arises from different S-P transitions [20]. However, the luminescence of Bi ions usually appears in the visible wavelength region such as orange–red emission of B^{++} ions [21] and blue or green emission of B^{+++} ions [22], Furthermore, the visible emission band arised from an energy transfer among B^{+++} ions. Therefore, it can be said that the blue emission from the Bi_2O_3 nanowire is attributed to the presence of B^{+++} ions predominant in the β-Bi_2O_3 phase.

When an extremely thin ZnO layer (10 ALD cycles) was deposited on the Bi_2O_3 nanowire by using an ALD technique the broad violet emission peak due to the Bi_2O_3 nanowire has disappeared and a new green–yellow emission peak centered at around 560 nm due to the ZnO layer has appeared. As the number of ALD cycle increases from 10 to 20 a very small emission peak tends to appear at about 370 nm. Generally a PL emission spectrum from undoped ZnO has two emission bands: one is the ultraviolet near-band edge emission (NBE) and the other is green–yellow emission. The former is due to free exciton recombination, in other words, associated with the transition from the conduction band to the valence band, while the latter is due to deep level transition, associated with structural defects such as oxygen vacancies and zinc interstitials. For the number of ALD cycle less than 10 only green–yellow emission seems to be observed. The very small NBE peak for an ALD cycle of 20 may be attributed to the spontaneous emission from the free exciton. With continued increases in ALD cycle from 20 to 30, 40 and 50 the NBE peak rapidly increases. This rapid increase in the NBE peak height can be explained by exciton-exciton scattering process, in which one of the two excitons obtains energy from the other and scatters into a higher exciton energy state. The changing trend of PL emission spectrum tells us that it is not easy to control the wavelength of the emitted light from the Bi_2O_3-core/ZnO-shell 1D structure to fall in the range from 450 nm to 550 nm by changing the number of ALD cycle (or the thickness of the ZnO-shell). Since the wavelength of the main emission peak changes very abruptly with an increase in the number of ALD cycle.

4. Conclusions

Highly straight single crystal Bi_2O_3 nanowires with sizes of 50–300 nm in diameter and 50–100 in length were synthesized on Au-coated c–plane sapphire (Al_2O_3) substrates by thermal evaporation using Bi powders. One dimensional(1D) Bi_2O_3–core/ZnO-shell structures with uniform layer thicknesses were subsequently prepared by coating the Bi_2O_3 nanowires with ZnO using atomic layer deposition (ALD). The crystalline nature of the 1D core/shell structure was revealed by high resolution transmission electron diffraction(SAED). X–ray diffraction(XRD) results indicate that the Bi_2O_3-core is a pure tetragonal β-Bi_2O_3 phase single crystal, while the ZnO-shell is amorphous. EDS analysis confirms that the Bi_2O_3 nanowires grow via vapor–liquid–solid(VLS) mechanism in thermal evaporation of Bi powders. The photoluminescence(PL) spectra of the 1D core/shell structures show that a violet emission at ∼450 nm characteristic of Bi_2O_3 changes to UV and green–yellow emissions at 370 and 590 nm, respectively, characteristic of ZnO very abruptly within 10 cycles as the number of ALD cycles increases.

Acknowledgment

This work was supported by Korean Science and Engineering Foundation (KOSEF) through '2007 National Research Laboratory Program'.

References

[1] B. Liu, H.C. Zeng, J. Phys. Chem. B 108 (2004) 5867.
[2] L.J Lauhon, M.S. Gudilesen, C.M. Lieber, Phil. Trans. R. Soc. Lond. A 362 (2004) 1247.
[3] See, for example, E.Y. Wang, K.A. Pandelisev, J. Appl. Phys. 52 (1981) 4818.
[4] See, for example, N.X. Jiang, E.D. Wachsman, J. Am. Ceram. Soc. 82 (1999) 3054.
[5] See, for example, C.C. Huang, K.Z. Fung, Mater. Res. Bull. 41 (2006) 1604.
[6] R. Becker, W. Doring, Ann. Phys. 24 (1935) 719.
[7] S.K. Blower, C. Greaves, Acta Crystallogr. C 44 (1935) 587.
[8] A F Gualtieri, S Immovilli, M Prudenziatiy, Power Diffract. 12 (1997) 90.
[9] P. Shuk, H.D. Wiemhofer, V. Guth, Wo Gopel, M. Greenblatt, Solid State Ion. 89 (1996) 179.
[10] A.N. Romanov, D.P. Shashkin, E.V. Khaula, J. Russ 2000 Inorg. Chem. 45 (2000) 500.
[11] Q. Yang, Y. Li, Q. Yin, P. Wang, Y.-B. Cheng, Mater. Lett. 55 (2002) 46.
[12] T.P. Gujar, V.R. Shinde, C.D. Lokande, S.-H. Han, Mater. Sci. Eng. B 133 (2006) 177.
[13] H.Y. Kim, J.H. Myung, S.H. Shim, Solid State Commun. 133 (2006) 177.
[14] X.-P. Shen, S.-K. Wu, H. Zhao, Q. Liu, Physica E 39 (2007) 133.
[15] L. Leontie, M. Caraman, M. Alexe, C. Harnagea, Surf. Sci. 480 (2002) 507.
[16] Y. Qiu, D. Liu, J. Yang, S. Yang, Adv. Mater. 18 (2006) 2604.
[17] L. Kumari, J.-H. Lin, Y.-R. Ma, Nanotechnol. 18 (2007) 295605.
[18] W. Dong, C. Zhu, J. Phys. Chem. Solids 64 (2004) 265.
[19] L. Kumari, J.-H. Lin, Y.-R. Ma, Nanotechnol. 18 (2007) 295605.
[20] A.M. Srivastava, W.W. Beers, J. Lumin. 80 (1999) 293.
[21] G. Blasse, J. Phys. Chem. Solids 55 (1994) 171.
[22] S. Parke, R.S. Webb, J. Phys. Chem. Solids 34 (1973) 85.